Group-III-Nitride Superluminescent Diodes for Solid-State Lighting and High-Speed Visible Light Communications

Chao Shen, *Member, IEEE*, Jorge A. Holguin-Lerma, *Student Member, IEEE*, Abdullah A. Alatawi, *Student Member, IEEE*, Peng Zou, Nan Chi, *Member, IEEE*, Tien Khee Ng, *Senior Member, IEEE*, and Boon S. Ooi, *Senior Member, IEEE*

***Abstract*—Group-III-nitride superluminescent diodes (SLDs) are emerging as light sources for white lighting and visible light communications (VLC) owing to their droop-free, low speckle noise, and large modulation bandwidth properties. In this paper, we discuss the development of GaN-based visible SLDs, and analyze their electro-optical properties by studying the optical power-bandwidth products and injection current densities. The significant progress in blue SLDs and their applications for white light VLC is highlighted. A blue SLD, with an optical power of >100 mW and large PBP of 536 mW·nm, is utilized to generate white light, resulting in a high color rendering index (CRI) of 88.2. In a modulation experiment designed for an SLD-based VLC system, an on–off keying scheme exhibits a 1.2 Gbps data rate, with a bit error rate of 1.8 $\times 10^{-3}$, which satisfies the forward error correction criteria. A high data rate of 3.4 Gbps is achieved using the same SLD transmitter, by applying the 16-quadrature-amplitude-modulation (16-QAM) discrete multitone modulation scheme for high-speed white light communication. The results reported here unequivocally point to the significant performance and versatility that GaN-based SLDs could offer for beyond-5G implementation, where white lighting and high spectral efficiency VLC systems can be simultaneously implemented.**

***Index Terms*—Amplitude modulation, gallium nitride, laser diodes, solid-state lighting, superluminescent diodes, visible light communication.**

I. Introduction

THE development of group-III-nitride optoelectronic devices is essential for many important applications, such as solid-state lighting (SSL), full-color display, optical data storage, projection, and medical diagnosis [1]. Energy-efficient white lighting technology could not be realized without the invention and development of GaN-based light emitters [2]. Violet-blue light-emitting diodes (LEDs) have been widely accepted as the building block for white light bulbs, and blue laser diodes (LDs) have also been investigated for high-intensity, droop-free light sources [3], [4]. The group-III-nitride superluminescent diode, sometimes denoted as an SLD or SLED, is an emerging type of light emitter that has attracted increasing attention [5]. Since first appearing in 2009 [6], group-III-nitride SLDs have undergone steady improvement in terms of the output power, optical bandwidth, and emission at different wavelengths [7].

Group-III-V SLDs in the near-infrared (NIR) wavelength domain have been studied since the first GaAs-based SLDs were introduced in the 1970s [8], [9]. These SLDs are based on compounds and alloys formed by elements such as In, Ga, Al, As, P, and Sb. Subsequently, SLDs at ∼830 nm, ∼1.3 μm, and ∼1.55 μm have been demonstrated, and SLDs based on quantum dots [10]–[13], quantum dashes [14]–[16], and quantum wells [17], [18] have been investigated. NIR SLDs have taken up an important role in medical technology, such as in the optical coherence tomography (OCT) [19], [20]. Recently, the strain-induced quantum well intermixing technique was utilized in an InGaP/InAlGaP system to obtain a yellow-emitting SLD [21], [22], which is the shortest wavelength achievable in a conventional III/V material system. Hence, the development of group-III-nitride SLDs has become essential to obtaining short wavelength SLDs, including near-ultraviolet (UV), blue and green SLDs.

Group-III-nitride SLDs are optical devices operating at amplified spontaneous emission (ASE). This allows them to emit a high-brightness, broad spectral bandwidth, and low temporal coherence output beam within a single or double pass of gain over a wide spectral range [23]. The SLD structure is similar to the Fabry-Pérot LD, but without an intrinsic resonant cavity, i.e., inhibition of optical feedback is intentionally implemented. The GaN-based SLD has become a potential candidate for a high-performance light source mainly owing to its high power and broader emission bandwidth.

Manuscript received February 1, 2019; revised April 1, 2019; accepted April 29, 2019. Date of publication May 13, 2019; date of current version June 24, 2019. This work was supported in part by the King Abdulaziz City for Science and Technology under Grant KACST TIC R2-FP-008 and in part by the King Abdullah University of Science and Technology (baseline funding, BAS/1/1614-01-01, KAUST funding KCR/1/2081-01-01, REP/1/2878-01-01, and GEN/1/6607-01-01). *(Corresponding author: Boon S. Ooi.)*

C. Shen, J. A. Holguin-Lerma, A. A. Alatawi, T. K. Ng, and B. S. Ooi are with the Photonics Laboratory, King Abdullah University of Science and Technology, Thuwal 21534, Saudi Arabia (e-mail: chao.shen@kaust.edu.sa; jorge.holguinlerma@kaust.edu.sa; abdullah.atawi@kaust.edu.sa; tienkhee.ng@kaust.edu.sa; boon.ooi@kaust.edu.sa).

P. Zou and N. Chi are with the Shanghai Institute for Advanced Communication and Data Science, Key Laboratory for Information Science of Electromagnetic Waves (MoE), Fudan University, Shanghai 200086, China (e-mail: 18110720058@fudan.edu.cn; nanchi@fudan.edu.cn).

Color versions of one or more of the figures in this paper are available online at http://ieeexplore.ieee.org.

Digital Object Identifier 10.1109/JSTQE.2019.2915995

This work is licensed under a Creative Commons Attribution 3.0 License. For more information, see http://creativecommons.org/licenses/by/3.0/

The rapid expansion of visible light communication (VLC) at the present time is an important driving force for the research and development of GaN-based blue SLDs [24], [25]. VLC has gained huge interest for transmitting multi-gigabit-per-second data without electromagnetic interference (EMI) [26]–[28]. Hence, VLC-based technology enables high-speed networks in radio frequency (RF) sensitive areas, such as hospitals and aircrafts. In SSL-VLC systems, high-brightness and high-speed light emitters are required. GaN-based LDs have been employed in SSL-VLC systems, owing to their large modulation bandwidth, and Gbps data rates have been reported using on-off keying (OOK) [29], and orthogonal frequency division multiplexing (OFDM) modulation techniques [30]. Such systems also find unique applications in underwater wireless optical communication [31], [32]. We recently demonstrated the utilization of a GaN-based SLD as an alternative light source for SSL-VLC systems [25], which offers high output power and "efficiency-droop"-free characteristics as a compact optical transmitter. Moreover, shorter-wavelength SLDs play a major role in achieving the in-plane resolutions and signal detection enhancements necessary for imaging applications [33].

In this study, we further discuss the design of a high-power blue-emitting SLD and its corresponding electro-optical properties. A comparison of the performances of reported GaN SLDs is presented for the first time, with a focus on the output power and optical bandwidth. The feasibility of implementing GaN-based SLDs for white-light and VLC is further reinforced. A data rate beyond Gbps is achieved based on OOK modulation scheme, and a record data rate of 3.4 Gbps is demonstrated using the spectral-efficient quadrature- amplitude-modulation (QAM) discrete-multitone (DMT) technique.

II. Electro-Optical Properties of III-Nitride SLDs

A. High-Power Blue SLD

GaN-based SLDs have similar epitaxial structures to LDs but with a different waveguide or facet configuration to suppress the formation of resonance cavities. This can be achieved by various approaches, including antireflection (AR) facet coating [34], facet roughening [35], utilizing a passive absorber [25], [36], waveguide bending [37]–[40], and tilted facets [6], [7], [34], [41], [42]. Here, we fabricated a blue-emitting SLD featuring a 12° tilted-facet design on a c-plan GaN substrate, with a $\sim$1-mm cavity length. The epitaxial structure consists of AlGaN cladding layers, InGaN/GaN multiple quantum wells as active region, highly doped GaN contact layer and AlGaN electron blocking layer. The waveguide width is 15 μm. The fabrication process has been discussed in detail elsewhere [43].

For a single-pass SLD, the optical power can be defined as,

$$P \approx P_{sp}\, G_s\,(j, L)\,, \tag{1}$$

where P_{sp} is the spontaneous emission power, and G_s is the single-pass optical gain. G_s is a function of the current density (j) and cavity length (L), and is given by:

$$G_s\,(j, L) = \exp\left[\left(\Gamma g_o \eta \frac{j}{d} - \alpha\right) L\right], \tag{2}$$

where Γ is the confinement factor, g_o is the gain coefficient, η is the internal quantum efficiency, d is the active layer thickness and α is the absorption coefficient [44].

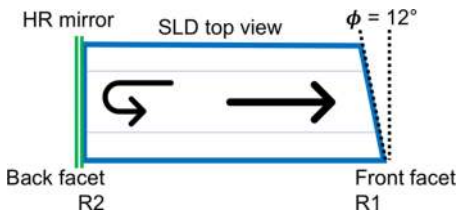

Fig. 1. Schematic of the fabricated double-pass SLD with an HR-coated back facet and 12° tilted front facet.

In a single-pass SLD, the reflectivity of the front and back facets should be as small as possible, which can be achieved by AR coating. However, in this case, the device requires a significantly large single-pass gain (G_s) to achieve high-power output, which calls for a high injection current density (j), and a long cavity length (L) [44]. A higher injection inadvertently leads to joule heating, and a device with a long cavity length may not be efficient. A preferred device design for achieving high-power SLD is based on a double-pass configuration, in which a high-reflective (HR) mirror $(R_2 > 0.9)$ is coated at the back facet [39]. In a double-pass SLD, the output power is proportional to the square of the gain, as

$$P \approx P_{sp}\, R_2\, G_s^2. \tag{3}$$

For a given $R_2 > 0.9$, the front facet reflectivity (R_1) should be kept as small as possible, to minimize the generation of spectral modulation, which is undesirable for SLDs due to its impact to the coherence properties of SLD [44]. This challenge can be solved by tilting the waveguide or facet beyond a certain angle. A modal reflectivity below 10^{-6} can be achieved in SLDs with facet angles greater than 6° [45], [46]. Our SLD features a 12° tilted facet, in conjunction with an HR-coated back facet mirror, as shown in Fig. 1.

Fig. 2 depicts the optical power *vs.* current (*L-I*) and voltage *vs.* current (*V-I*) relations of a blue-emitting SLD operating under the CW condition at room temperature. The external quantum efficiency (EQE) and the injection current density are also shown. The device was measured using the Keithley 2520 laser diode testing system with a calibrated Si photodetector. The device has an output optical power of $\sim$105 mW at 1 A, as shown in Fig. 2. A superlinear increase in the L-I curve is observed following the onset of superluminescent characteristics, at approximately $\sim$500 mA, with an increasing EQE observed in the ASE regime. The SLD has a relatively low operating voltage of 4.38 $\sim$ 4.78 V at a current of 500 $\sim$1000 mA, resulting in a low (dV/dI) series resistance ($\leq$1 Ω).

The electroluminescence (EL) spectra (Fig. 3) were measured using a Yokogawa AQ6373B optical spectrum analyzer, exhibiting peak emissions at $\sim$443 nm. A blue-shift in the emission peak

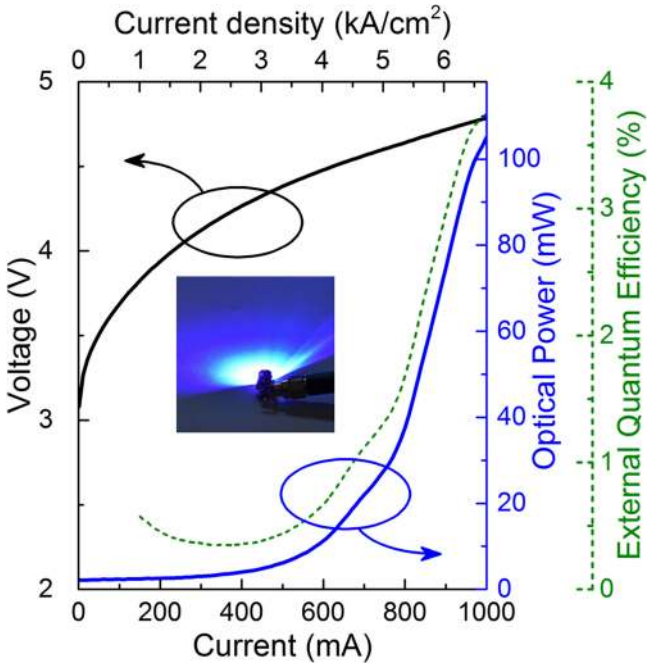

Fig. 2. Voltage *vs.* current and optical power *vs.* current relations of a blue-emitting SLD operating under the CW condition. The corresponding injection current density has been labeled. The green dot line refers to the external quantum efficiency (EQE) of the SLD. Inset: photo of the TO-can packaged, unmounted blue SLD.

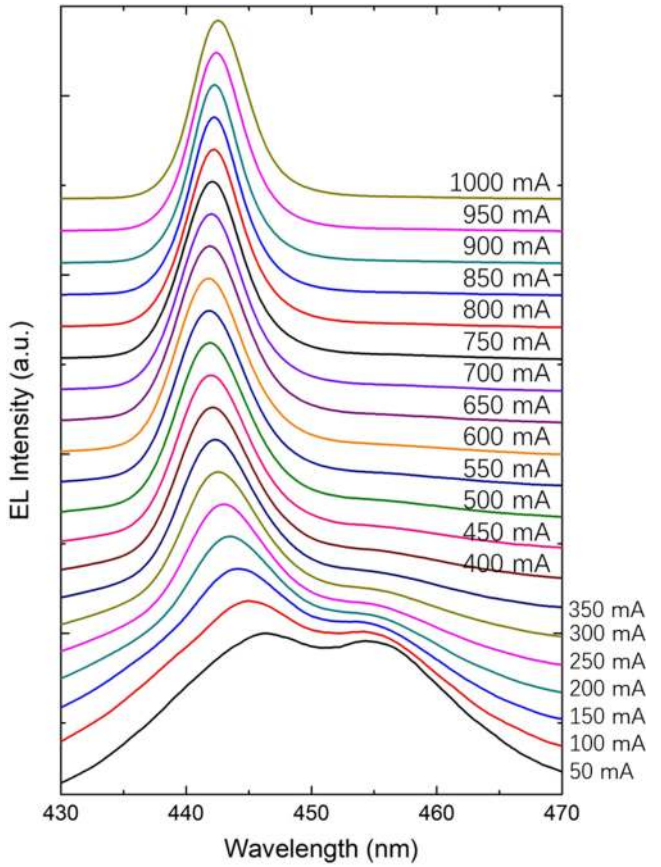

Fig. 3. EL spectra of the SLD under various injection currents. A decreasing FWHM is observed with an increasing current.

and reduction in the peak full-width at half-maximum (FWHM) can be observed with an increasing injection current. The blue shift may be attributed to the band filling effect. At 50 mA, the FWHM of the EL peak is 26.3 nm, which reduces to 7.25 nm at an injection current of 500 mA. A reduced red-shift ($<$0.75 nm) is observed at current values over 600 mA, owing to the self-heating effect during CW operation. The SLD emission maintains a relatively large peak FWHM of 5.1 nm at a high injection current of 1000 mA. Such a large FWHM, *i.e.,* a broad optical bandwidth, makes the SLD promising for lighting, projection, and spectroscopy applications.

B. Comparative Review of Electro-Optical Properties of GaN-Based SLDs

Many parameters are relevant to the electro-optical properties of SLDs, including the optical power (mW), optical bandwidth (nm), peak wavelength (nm), injection current (mA), and current density (kA/cm^2). Because enhancing the power-bandwidth product (PBP) of SLD devices is of prime importance, here we evaluate the PBPs from SLDs with different designs and configurations. Table I summarizes the electro-optical properties of the reported GaN-based SLDs in terms of the optical power, optical bandwidth, PBP, current density, and pulsed/CW operation. For our current device, the PBP is 536 mW·nm at 1000 mA. To provide a fair comparison of the reported devices, we compare the peak PBP and the injection current density, as shown in Fig. 4a. The results for which the SLD was driving under pulsed or CW condition are labelled differently. Of all the reported devices we reviewed, the highest PBP is 931.7 mW·nm, calculated based on an optical power of 121 mW and a peak FWHM of 7.7 nm at 9.5 kA/cm^2, from a 446-nm-emitting SLD grown on a semipolar GaN substrate with a passive absorber design operating in CW mode reported in 2017 [54]. Other SLDs showing a PBP of $>$ 650 mW·nm include a 447-nm-emitting semipolar SLD, with a PBP of 775 mW·nm at 8 kA/cm^2 [25]; a 429-nm-emitting SLD, with a PBP of 700 mW·nm at 15 kA/cm^2 [5]; and a 442-nm-emitting SLD, with a PBP of 682.5 mW·nm at 6.7 kA/cm^2 [7]. A higher PBP is partially attributed to a higher optical power, where an SLD with a higher material gain is favored.

Next, we consider the ratio of the PBP to the current density ((mW·nm)/(kA/cm^2)). This ratio provides a measure of how efficiently electrical charges are converted into optical power along a determined optical bandwidth. Fig. 4b presents the PBP over the current density *vs.* the emission wavelength for the reported devices. The highest PBP to current density value reported is 101.87 (mW·nm)/(kA/cm^2), for a blue SLD using a tilted facet configuration on a *c*-GaN substrate [7]. This is result of the high quantum efficiency in this SLD originating from the high-quality active region in the epitaxial layers. Our previously presented semipolar SLDs also exhibit high values in terms of the PBP to current density value, such as $\sim$98 (mW·nm)/(kA/cm^2) in [54]

TABLE I
ELECTRO-OPTICAL PROPERTIES OF III-NITRIDE SLDS

λ (nm)	P (mW)	FWHM (nm)	PBP (mW·nm)	J (kA/cm2)	Pulsed / CW	Year	Ref.
392	70	2.1	147	10.9	CW	2013	[47]
392	320	/	/	33.2	Pulsed	2013	[47]
405	200	3	600	/	CW	2011	[48]
405	350	/	/	/	CW	2016	[37]
405	125	2.5	312.5	16.7	CW	2012	[36]
405	20	9	180	16.9	CW	2016	[41]
405	0.65	5.23	3.4	19	Pulsed	2010	[42]
407-416	3	15.5	46.5	8.3	CW	2017	[49]
408	230	2.5	575	/	CW	2013	[38]
409	170	2.5	425	13.3	CW	2015	[46]
412	55	/	/	17.5	Pulsed	2010	[34]
412	39	4.5	175.5	12.5	CW	2010	[34]
417	14	5.1	71.4	36	Pulsed	2015	[50]
420	100	/	/	39.4	Pulsed	2009	[6]
420	2.8	4.6	13	15.6	CW	2009	[6]
422	2	5	10	16.7	CW	2016	[33]
426	12	10	120	8.9	Pulsed	2017	[51]
429	70	10	700	15	Pulsed	2017	[5]
429	1	3	3	/	Pulsed	2018	[52]
439	5	9	45	15.8	Pulsed	2009	[35]
440	150	4	600	/	CW	2018	[53]
442	474	/	/	6.7	Pulsed	2018	[7]
442	105	6.5	682.5	6.7	CW	2018	[7]
443	105	5.1	536	6.7	CW	2019	[*]
444	105	2.6	273	15.4	CW	2013	[39]
446	121	7.7	931.7	9.5	CW	2017	[54]
447	250	2.2	550	9.3	CW	2016	[25]
447	123	6.3	775	8	CW	2016	[25]
500	20	10	200	/	Pulsed	2018	[55]
500	4.3	4.4	17.6	18.8	CW	2012	[40]
505	1	10	10	/	Pulsed	2018	[56]
526	1.06	26	27.6	/	CW	2019	[57]

P refers to the optical power from the SLD, FWHM refers to the optical bandwidth of the emission peak, PBP refers to the power-bandwidth product, J refers to the injection current density, and "∗" refers to the results presented in this work.

and 59 ∼ 97 (mW·nm)/(kA/cm^2) in [25], suggesting that such devices are promising for high-brightness light emitters.

Fig. 4c evaluates the reported optical powers across different wavelengths for the considered SLDs. Most of the SLDs we developed are blue-emitting devices (∼450 nm), making them suitable for SSL, pico-projection, and VLC applications. The highest optical power reported for III-nitride SLDs operating in CW mode is 350 mW, in a 405-nm-emitting "j-shape" curved waveguide SLD on a *c*-GaN substrate [37]. A blue SLD with a recorded optical power of 474 mW in pulse mode was reported in [7]. There have been significant efforts to develop high-power SLDs in violet (∼405 nm) and blue (∼450 nm), with reported optical powers exceeding 200 mW. However, GaN-based SLDs in the cyan-green color regime still exhibit low optical powers, which is known as the "green-gap" valley. Currently, the optical powers for reported SLDs with emission wavelengths over 460 nm are 4.3 mW in CW mode [40] and 20 mW in pulse mode [55]. Intense efforts are required to further improve the optical power of cyan-green SLDs.

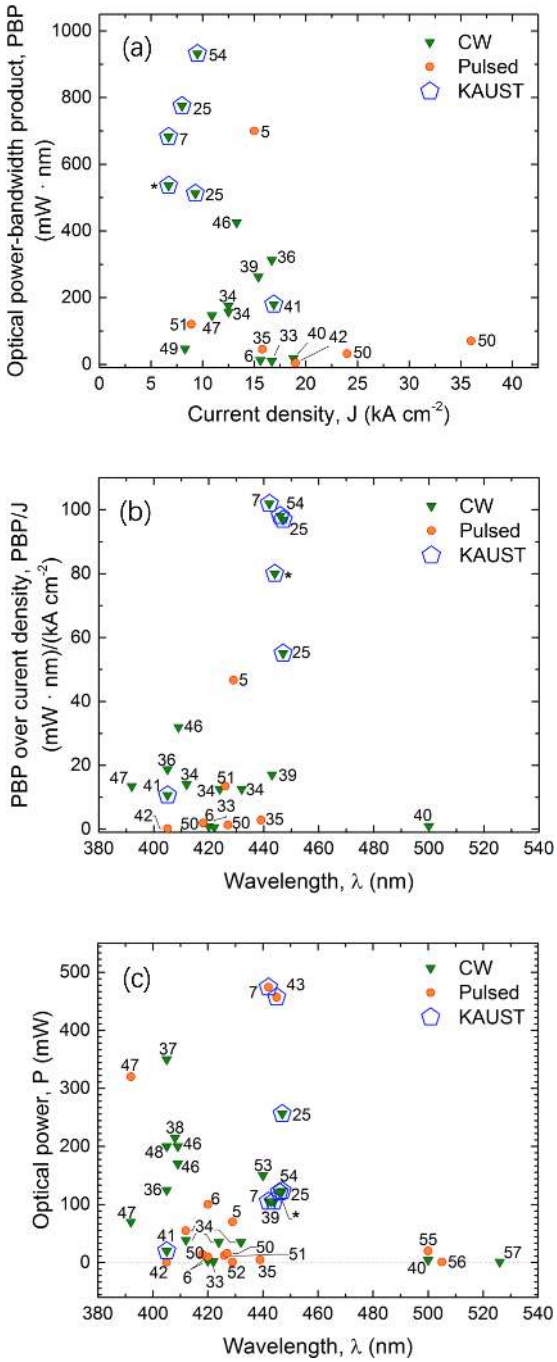

Fig. 4. Plots of (a) PBP *vs.* current density, (b) PBP over current density *vs.* wavelength, and (c) optical power *vs.* wavelength in GaN-based SLDs reported in prior work. The numbers correspond to the references in which the data points were obtained. The results from SLDs operating in pulsed and CW mode have been labelled separately, and the performances of SLDs reported from KAUST Photonics Laboratory have been highlighted. "∗" refers to the results presented in this work.

III. SLD-BASED WHITE LIGHTING

White light can be generated using violet-blue light emitters exciting one or multiple phosphors as color converters [58]. A comparison of the spectra, chromatic properties, and emission patterns in white light generated using LEDs, SLDs,

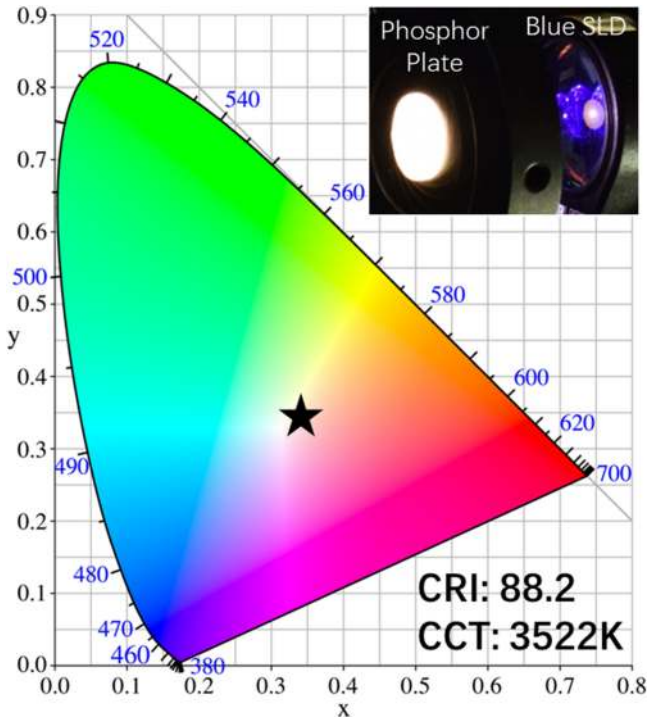

Fig. 5. Plot of chromaticity coordinates at (0.38, 0.35) on CIE 1931 color space for the SLD generated white light. Inset: photo of the white light generated using blue SLD exciting phosphor plate.

and LDs in this configuration was provided in [54]. Compared with white LEDs, LD- and SLD-based white light bulbs have potential advantages including circumventing the "efficiency droop" to achieve a high efficiency at high input power densities, a requirement for less phosphor material, smaller device sizes, and compact luminaire form factors [4], [59]. One of the key advantages of SLD over LD is its low coherence, which generates less speckle pattern, and thus makes the illumination more comfortable when perceived through human eyes, even without diffuse optics [5]. Thus, light bulbs based on blue SLDs face fewer safety issues compared with LD based light sources.

Combining blue LED or LD with YAG:Ce phosphor for white lighting has been widely demonstrated [29], [59], [60]. For example, employing a blue LD exciting a YAG:Ce phosphor crystal results in a white light with a color-rendering index (CRI) of 58 and color temperature (CCT) of 4740 K [29]. Similarly, using a blue SLD-exciting yellow phosphor, we obtained a white light with a CRI of 68.9 and CCT of 4340 K [25]. The improvement in the CRI results from the larger optical bandwidth of blue SLDs compared to blue LDs. Hence, SLDs with larger PBPs are advantageous for SSL applications.

To further improve the CRI for high-quality white lighting, a phosphor plate combining green and red phosphors can be employed in place of the yellow phosphor. By utilizing a blue SLD exciting the phosphor plate, a white light with high CRI of 88.2 has been obtained, as shown in Fig. 5. The CCT is 3522 K, which represents a warm white light. The corresponding Commission Internationale de l'Eclairage (CIE 1931) chromaticity coordinates at (0.38, 0.35) have been measured using a GL Spectis 5.0 Touch spectrometer and are plotted in Fig. 5. These results confirm that GaN-based SLDs can be integrated into indoor lighting systems, offering a desirable CRI. A higher CRI can be achieved by further engineering the phosphor mixture, such as adding more color conversion elements in the green, cyan and red color regime.

IV. SLD as Transmitter for VLC

While LEDs have been well-studied as transmitters in VLC systems, owing to their wide availability, their relatively small modulation bandwidth limits the data transmission rate in LED-based VLC systems [26]. Hence, many researchers have proposed different schemes to address this challenge. For example, a hardware equalizer that suppresses the low-frequency domain SNR to compensate for the high-frequency response can broaden the LED bandwidth, thus enabling an LED-based VLC system to achieve higher data rate [61], [62].

In our previous work, we demonstrated a GaN-based SLD exhibiting a significantly higher 3-dB modulation bandwidth, thus making it attractive for use as a transmitter in VLC systems. A blue-emitting SLD on a semipolar GaN substrate exhibits a modulation bandwidth of ∼500 MHz [54]. In a subsequent report, a 405-nm emitting semipolar SLD exhibited a bandwidth of up to 807 MHz [41]. For a high-power blue SLD on a *c*-GaN substrate, a modulation bandwidth of ∼400 MHz has recently been reported [7]. In this section, we study the performance of VLC systems based on blue SLD transmitters, and investigate the system performance using various modulation techniques, *i.e.*, OOK and DMT.

A. OOK Modulation

Non-return-to-zero OOK (NRZ-OOK) modulation has been widely employed in VLC systems, owing to its low complexity. To study the data transmission capability of an SLD-based VLC system, we employ a pseudorandom binary sequence (PRBS) 2^{10}-1 data stream generated by the Agilent N4903B J-BERT pattern generator. A data transmission experiment is conducted by measuring the bit error rates (BERs) and eye diagrams at different data rates (Fig. 6). The setup also involves a PSPL5866 linear amplifier, PSPL5580 bias tee, and 1-GHz APD210 Si avalanche photodetector as the receiver. The eye diagrams are collected using a DCA-86100C digital communication analyzer and are depicted in Figs. 6b and 6c. A data rate of 1.2 Gbps was achieved with a BER of 1.8×10^{-3}, which is below the forward error correction (FEC) limit of 3.8×10^{-3}. The corresponding eye diagram (Fig. 6c) shows open eyes at 1.2 Gbps, demonstrating that GaN-based SLDs can be utilized as high-speed transmitters in VLC systems.

B. DMT Modulation

To achieve a higher data rate, high spectral efficiency (SE) modulation formats such as orthogonal frequency division multiplexing (OFDM) and discrete multi-tone (DMT), have been demonstrated for optical wireless communications [62]–[64]. In

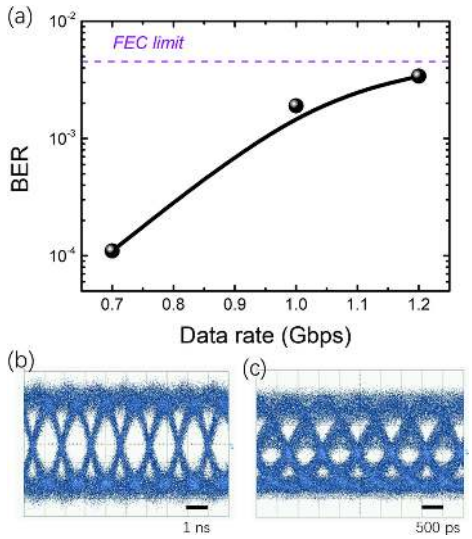

Fig. 6. (a) Plot of BER *vs.* data rate for SLD-based VLC system using NRZ-OOK modulation technique. (b) Eye diagram of the VLC system at 700 Mbps. (c) Eye diagram of the VLC system at 1.2 Gbps.

addition, high-speed VLC links based on DMT utilizing a phosphorescent white LED as a transmitter have been demonstrated [65], [66]. Advanced modulation formats such as carrier-less amplitude and phase (CAP) and OFDM can also help to improve the system performance in an LED-based VLC system [63], [67]. Moreover, QAM and wavelength division multiplexing (WDM) might enable a high-speed VLC system based on RGB LEDs [68].

In this study, we employ the 16-QAM-DMT modulation scheme to evaluate the system performance of an SLD-based VLC system for the first time. In this DMT modulation technique, we denote the discrete time domain signal by $s(n)$ and discrete frequency domain signal by $S(k)$. Then, the discrete time domain symbol of DMT can be expressed as [69]

$$s\left(n\right)=\frac{1}{N}\sum_{k=0}^{N-1}S\left(k\right)F_N^{-kn},\ n=0,1,\ldots,N-1 \tag{4}$$

where $F_N^{-kn}=\exp(-\mathrm{j}\frac{2\pi}{N}\mathrm{kn})$, and N is the total number of DFT or IDFT points. The discrete frequency domain signal can be written as:

$$S\left(k\right)=S_r\left(k\right)+S_i\left(k\right)\cdot j \tag{5}$$

where $S_r(k)\,\text{and}\,S_i(k)$ are the real and the imaginary parts of $S(k)$, respectively. Then (4) can be written as:

$$\begin{aligned}s\left(n\right)=\frac{1}{N}\sum_{k=0}^{N-1}&(S_r\left(k\right)+S_i\left(k\right)\cdot j)\cdot\left(\cos(-\frac{2\pi}{N}kn\right)\\&+j\cdot\sin\left(-\frac{2\pi}{N}kn\right)\Big)=\frac{1}{N}\sum\nolimits_{k=0}^{N-1}(S_r\left(k\right)\\&\cdot\cos\left(-\frac{2\pi}{N}kn\right)-S_i\left(k\right)\cdot\sin\left(-\frac{2\pi}{N}kn\right)\Big)\\&+\frac{1}{N}\sum_{k=0}^{N-1}\left(S_i\left(k\right)\cdot\cos(-\frac{2\pi}{N}kn\right)+S_r\left(k\right)\\&\cdot\sin\left(-\frac{2\pi}{N}kn\right)\Big)\cdot j=s_r\left(n\right)+s_i\left(n\right)\cdot j\end{aligned} \tag{6}$$

In the majority of cases, N is an even number. Thus, $s_i(n)$ can be written as:

$$\begin{aligned}s_i(n)=\frac{1}{N}\Bigg(&\sum_{k=0}^{N/2-1}\left(\left(S_i(k)\cdot\cos\left(-\frac{2\pi}{N}kn\right)+S_r\left(k\right)\right.\right.\\&\left.\left.\cdot\sin\left(-\frac{2\pi}{N}kn\right)\right)\cdot j+\sum_{k=N/2+1}^{N-1}\left(\left(S_i\left(k\right)\cdot\cos\left(-\frac{2\pi}{N}kn\right)\right.\right.\right.\\&\left.\left.\left.+\ S_r\left(k\right)\cdot\sin\left(-\frac{2\pi}{N}kn\right)\right)\cdot j\right)+\frac{1}{N}\left(-S_i\left(\frac{N}{2}\right)\right)\cdot j\\=\frac{1}{N}&\left(S_i(0)-S_i\left(\frac{N}{2}\right)\right)\cdot j+\frac{1}{N}\sum_{k=1}^{N/2-1}\left(S_r\left(k\right)\right.\\&-\left.S_r(N-1-k)\right)\cdot\sin\left(-\frac{2\pi}{N}kn\right)\cdot j+\frac{1}{N}\sum_{k=1}^{N/2-1}\left(S_i(k)\right.\\&+\left.S_i(N-1-k)\right)\cdot\cos\left(-\frac{2\pi}{N}kn\right)\cdot j\end{aligned} \tag{7}$$

From (7), we can conclude that if we want to obtain a real-valued time domain signal for the IDFT, then the complex signal of the frequency domain in a specific period N should satisfy the following relationship,

$$\begin{aligned}S\left(k\right)&=Q\left(k\right)\ k=1,2,\ldots,N/2-1\\S\left(k\right)&=Q'\left(N-k\right)\ k=N/2+1,\ldots,N-1\end{aligned} \tag{8}$$

where $Q(k)$ is the k$^{\text{th}}$ complex symbol of 16-QAM, and $Q'(k)$ is the conjugated complex data of $Q(k)$. In addition, $S(0)=S(\frac{N}{2})=0$. In practice, the 0 to (N/2–1)th subcarriers are placed on the positive frequency carriers, while the (N/2) to (N-1)th subcarriers are placed on the corresponding negative frequency carriers. If the QAM symbols satisfy the relationship depicted in (8), then we can obtain a real-valued time domain signal by the IDFT, which can be directly modulated on the blue SLD and received by the Si APD.

Fig. 7 illustrates the system structure. At the transmitting side, a decimal random data stream from 0–15 is mapped into 16-QAM symbols. The five lowest frequency subcarriers will be filled with zeros, owing to the low SNRs presented in these subcarriers. To transform the complex data into real-valued time domain data, we will conjugate the origin complex symbols and assemble them. Up-sampling can suppress the frequency spectrum and broaden the time domain signal, which improves the system performance. Then, after applying the IDFT the real-valued time domain signal is generated. A cycle prefix (CP) is employed to mitigate the multi-path effect. A Tektronix AWG7122C arbitrary waveform generator (AWG) was utilized in this experiment.

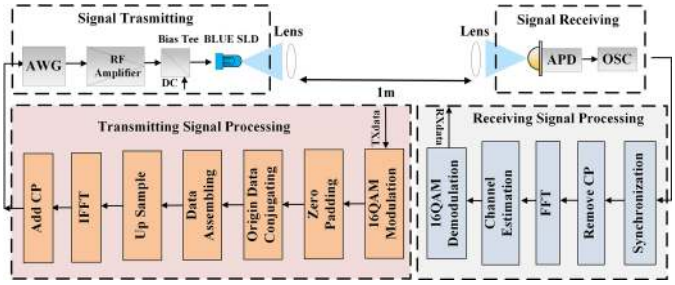

Fig. 7. Schematic structure of the SLD-based VLC system setup using the DMT modulation technique.

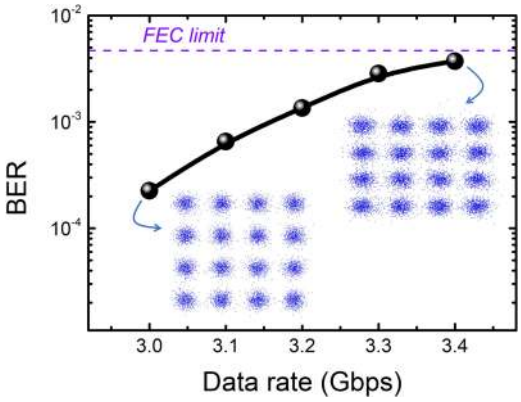

Fig. 8. Plot of the BER *vs.* data rate for an SLD-based VLC system using the 16-QAM-DMT modulation technique. Insets: corresponding constellations of the received signal at 3 Gbps and 3.4 Gbps.

At the receiving end, the received signal was synchronized and aligned with the transmitted signal. The CP is first removed, and after applying the DFT the signal is transformed to complex symbols in the frequency domain. Channel estimation equalizes the receiving complex symbols, which improves the system performance. Finally, the received 16-QAM complex symbols are demodulated, and the overall BER value is obtained. The BERs and corresponding constellation diagrams at 3 Gbps and 3.4 Gbps at different data rates are presented in Fig. 8.

At 3.4 Gbps, the SLD-based VLC system has a BER of 3.7×10^{-3}, which satisfies the FEC criteria of 3.8×10^{-3}. To the best of our knowledge, this is the first reported SLD-based VLC system with a data rate higher than 3 Gbps using the DMT modulation technique. Compared with LED-based VLC systems, such as a 513-Mbps VLC link based on DMT-modulation of a white LED [66], our system using SLD as the transmitter exhibits an attractive transmission data rate. A higher data rate of 1.6 Gbps has been achieved in an LED-based VLC system with a cascaded pre-equalization circuit [65]. Despite the fact that no hardware equalizers are utilized, the presented SLD-based VLC system enables a high-speed data link, owing to the high modulation bandwidth in the GaN-based SLDs. A higher data rate might be achieved by incorporating further improvements in the modulation technique. Bit-loading is one potential technique [70] for enhancing the performance of the SLD-based VLC link. The bit-loading capability of this SLD at various frequencies has been

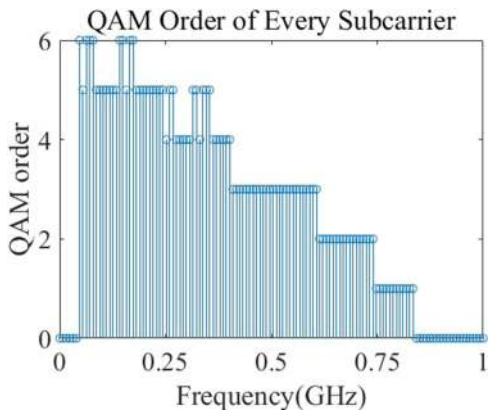

Fig. 9. Estimated QAM orders for each subcarrier for bit-loading scheme.

estimated using a DMT signal, where all subcarriers were modulated by binary phase-shift keying (BPSK) with an equal power. We illustrate the achievable QAM order against the frequency in Fig. 9. The first five subcarriers at the low-frequency end were intentionally set to zero. It should be noted that a number of subcarriers are capable of supporting 32-QAM DMT, with few of them supporting 64-QAM. Therefore, it is possible to achieve a higher system performance using SLD as the transmitter with bit- and power-loading DMT modulation techniques.

It is also worth mentioning that new types of group-III-nitride light emitters have also been developed recently showing potential in high-speed modulation, such as mini-LEDs, micro-LEDs and semipolar/nonpolar light emitters. For example, micro-LEDs show a maximum 3-dB bandwidth and optical powers of ∼500 MHz and ∼2 mW in [71], ∼800 MHz and $<$ 3 mW in [72], and ∼1 GHz and ∼1.7 mW in [73], respectively. Reported semipolar/nonpolar light emitters show a bandwidth and power of ∼1 GHz and ∼1.5 mW in [25], ∼1.5 GHz and ∼1.3 mW in [74], and ∼2.5 GHz and ∼2 mW in [52], respectively. Although many reports show relatively large modulation bandwidth, their low optical powers, which are way below 10 mW, limit the practical application in white-lighting and long-range VLC systems [75]. Although most of the devices mentioned above are unpackaged devices, it may need further researches in improving the light extraction efficiency and utilizing arrayed micro-LEDs to enhance the output power for VLC applications.

V. Conclusion

Emerging VLC and simultaneous lighting applications require high-brightness and high-speed group-III-nitride light emitters. GaN-based superluminescent diodes offer considerable competitive advantages over LEDs and LDs. In this study, we have discussed the design and electro-optical properties of GaN-based SLDs for the abovementioned purpose. A blue SLD with $>$100 mW optical power operating in CW has been presented, exhibiting a large PBP of 536 mW·nm. The demonstrated device offers a benchmark towards the development of Watt-level violet-blue SLDs for matching the optical power reported in high-power LDs [76]. By combining the blue SLD

with phosphor, white-light with a CRI of 88.2 has been produced. The SLD-based VLC system offers a high data rate of 1.2 Gbps using the OOK technique, and an extended data rate of 3.4 Gbps using the DMT technique. This work highlights the competitive advantages of GaN-based SLDs in conjunction with the spectral-efficient QAM-DMT scheme for high-speed white-light communication beyond 5G.

REFERENCES

[1] S. Nakamura, S. Pearton, and G. Fasol, *The Blue Laser Diode: The Complete Story*. New York, NY, USA: Springer, 2000.

[2] S. Nakamura and M. R. Krames, "History of gallium-nitride-based light-emitting diodes for illumination," *Proc. IEEE*, vol. 101, no. 10, pp. 2211–2220, Oct. 2013.

[3] M. T. Hardy *et al.*, "Group III-nitride lasers: A materials perspective," *Mater. Today*, vol. 14, no. 9, pp. 408–415, Sep. 2011.

[4] J. J. Wierer, J. Y. Tsao, and D. S. Sizov, "Comparison between blue lasers and light-emitting diodes for future solid-state lighting," *Laser Photon. Rev*., vol. 7, no. 6, pp. 963–993, Nov. 2013.

[5] G. R. Goldberg *et al.*, "Gallium nitride superluminescent light emitting diodes for optical coherence tomography applications," *IEEE J. Sel. Topics Quantum Electron.*, vol. 23, no. 6, Nov./Dec. 2017, Art. no. 2000511.

[6] E. Feltin *et al.*, "Broadband blue superluminescent light-emitting diodes based on GaN," *Appl. Phys. Lett.*, vol. 95, no. 8, Aug. 24, 2009, Art. no. 081107.

[7] A. A. Alatawi *et al.*, "High-power blue superluminescent diode for high CRI lighting and high-speed visible light communication," *Opt. Express*, vol. 26, no. 20, pp. 26355–26364, Oct. 2018.

[8] L. Tien-Pei, C. Burrus, and B. Miller, "A stripe-geometry double-heterostructure amplified-spontaneous-emission (superluminescent) diode," *IEEE J. Quantum Electron.*, vol. 9, no. 8, pp. 820–828, Aug. 1973.

[9] L. N. Kurbatov *et al.*, "Investigation of superluminescence emitted by a gallium arsenide diode," *Sov. Phys. Semicond.*, vol. 4, no. 11, 1971, Art. no. 1739.

[10] H. S. Djie *et al.*, "InGaAs/GaAs quantum-dot superluminescent diode for optical sensor and imaging," *IEEE Sensors J*., vol. 7, no. 1-2, pp. 251–257, Jan./Feb. 2007.

[11] C. E. Dimas, H. S. Djie, and B. S. Ooi, "Superluminescent diodes using quantum dots superlattice," *J. Cryst. Growth*, vol. 288, no. 1, pp. 153–156, Feb. 2, 2006.

[12] S. Chen *et al.*, "GaAs-based superluminescent light-emitting diodes with 290-nm emission bandwidth by using hybrid quantum well/quantum dot structures," *Nanoscale Res. Lett.*, vol. 10, no. 1, Aug. 25, pp. 340-1–340-8, 2015.

[13] Z. Y. Zhang *et al.*, "Self-assembled quantum-dot superluminescent light-emitting diodes," *Adv. Opt. Photon.*, vol. 2, no. 2, pp. 201–228, 2010.

[14] M. Z. M. Khan, T. K. Ng, and B. S. Ooi, "Self-assembled InAs/InP quantum dots and quantum dashes: Material structures and devices," *Prog. Quant. Electron.*, vol. 38, no. 6, pp. 237–313, Nov. 2014.

[15] B. S. Ooi *et al.*, "Quantum dashes on InP substrate for broadband emitter applications," *IEEE J. Sel. Topics Quantum Electron.*, vol. 14, no. 4, pp. 1230–1238, Jul./Aug. 2008.

[16] H. S. Djie, C. E. Dimas, and B. S. Ooi, "Wideband quantum-dash-in-well superluminescent diode at 1.6 mu m," *IEEE Photon. Technol. Lett.*, vol. 18, no. 13–16, pp. 1747–1749, Jul./Aug. 2006.

[17] M. Z. M. Khan *et al.*, "High-power and high-efficiency 1.3-mu m superluminescent diode with flat-top and ultrawide emission bandwidth," *IEEE Photon. J.*, vol. 7, no. 1, Feb. 2015, Art. no. 1600308.

[18] D. S. Mamedov, V. V. Prokhorov, and S. D. Yakubovich, "Broadband radiation sources based on quantum-well superluminescent diodes emitting at 1550 nm," *Quantum Electron*., vol. 33, no. 6, pp. 511–514, Jun. 2003.

[19] P. H. Tomlins and R. K. Wang, "Theory, developments and applications of optical coherence tomography," *J. Phys. D. Appl. Phys.*, vol. 38, no. 15, pp. 2519–2535, Aug. 7, 2005.

[20] P. D. L. Greenwood *et al.*, "Quantum dot superluminescent diodes for optical coherence tomography: Device engineering," *IEEE J. Sel. Topics Quantum Electron.*, vol. 16, no. 4, pp. 1015–1022, Jul. /Aug. 2010.

[21] A. A. Al-Jabr *et al.*, "Large bandgap blueshifts in the InGaP/InAlGaP laser structure using novel strain-induced quantum well intermixing," *J. Appl. Phys.*, vol. 119, no. 13, Apr. 7, 2016, Art. no. 135703.

[22] M. A. Majid *et al.*, "First demonstration of InGaP/InAlGaP based 608nm orange laser and 583nm yellow superluminescent diode," in *Proc. IEEE Photon. Conf.*, 2015, pp. 575–576.

[23] M. Rossetti *et al.*, "Superluminescent light emitting diodes - the best out of two worlds," *Proc. SPIE*, vol. 8252, 2012, Art. no. 825208.

[24] Y. Guo *et al.*, "A tutorial on laser-based lighting and visible light communications: device and technology," *Chin. Opt. Lett.*, vol. 17, 2019, Art. no. 040601.

[25] C. Shen *et al.*, "High-brightness semipolar $(20\overline{2}1)$blue InGaN/GaN superluminescent diodes for droop-free solid-state lighting and visible-light communications," *Opt. Lett.*, vol. 41, no. 11, pp. 2608–2611, 2016.

[26] N. Chi, *LED-Based Visible Light Communications*. Berlin, Germany: Springer, 2018.

[27] F. Zafar, M. Bakaul, and R. Parthiban, "Laser-diode-based visible light communication: Toward gigabit class communication," *IEEE Commun. Mag.*, vol. 55, no. 2, pp. 144–151, Feb. 2017.

[28] N. Chi *et al.*, "Visible light communications: demand factors, benefits and opportunities," *IEEE Wireless Commun*., vol. 22, no. 2, pp. 5–7, Apr. 2015.

[29] C. Lee *et al.*, "2 Gbit/s data transmission from an unfiltered laser-based phosphor-converted white lighting communication system," *Opt. Express*, vol. 23, no. 23, pp. 29779–29787, Nov. 16, 2015.

[30] J. R. D. Retamal *et al.*, "4-Gbit/s visible light communication link based on 16-QAM OFDM transmission over remote phosphor-film converted white light by using blue laser diode," *Opt. Express*, vol. 23, no. 26, pp. 33656–33666, Dec. 28, 2015.

[31] H. M. Oubei *et al.*, "Light based underwater wireless communications," *Jpn. J. Appl. Phys.*, vol. 57, no. 8, Aug. 2018.

[32] C. Shen *et al.*, "20-meter underwater wireless optical communication link with 1.5 Gbps data rate," *Opt. Express*, vol. 24, no. 22, pp. 25502–25509, 2016.

[33] A. Kafar *et al.*, "Nitride superluminescent diodes with broadened emission spectrum fabricated using laterally patterned substrate," *Opt. Express*, vol. 24, no. 9, pp. 9673–9682, May 2, 2016.

[34] M. Rossetti *et al.*, "High power blue-violet superluminescent light emitting diodes with InGaN quantum wells," *Appl. Phys. Express*, vol. 3, no. 6, 2010, Art. no. 061002.

[35] M. T. Hardy *et al.*, "M-Plane GaN-based blue superluminescent diodes fabricated using selective chemical wet etching," *Appl. Phys. Express*, vol. 2, no. 12, Dec. 2009, Art. no. 121004.

[36] A. Kafar *et al.*, "Cavity suppression in nitride based superluminescent diodes," *J. Appl. Phys.*, vol. 111, no. 8, p. 083106, Apr. 15, 2012.

[37] A. Castiglia *et al.*, "GaN-based superluminescent diodes with long lifetime," *Proc. SPIE*, vol. 9748, 2016, Art. no. 97481V.

[38] A. Kafar *et al.*, "High-optical-power InGaN superluminescent diodes with "j-shape" waveguide," *Appl. Phys. Express*, vol. 6, no. 9, Sep. 2013, Art. no. 092102.

[39] F. Kopp *et al.*, "Blue superluminescent light-emitting diodes with output power above 100mW for picoprojection," *Jpn. J. Appl. Phys.*, vol. 52, no. 8, Aug. 2013, Art. no. 08JH07.

[40] F. Kopp *et al.*, "Cyan superluminescent light-emitting diode based on InGaN quantum wells," *Appl. Phys. Express*, vol. 5, no. 8, pp. 082105-1–082105-3, Aug. 2012.

[41] C. Shen *et al.*, "High-speed 405-nm superluminescent diode (SLD) with 807-MHz modulation bandwidth," *Opt. Express*, vol. 24, no. 18, pp. 20281–20286, 2016.

[42] K. Holc *et al.*, "Temperature dependence of superluminescence in InGaN-based superluminescent light emitting diode structures," *J. Appl. Phys.*, vol. 108, no. 1, Jul. 2010.

[43] A. A. Alatawi *et al.*, "High power GaN-based blue superluminescent diode exceeding 450 mW," in *Proc. IEEE Int. Semicond. Laser Conf.*, 2018, pp. 129–130.

[44] G. A. Alphonse, "Design of high-power superluminescent diodes with low spectral modulation," *Proc. SPIE*, vol. 4648, pp. 125–138, 2002.

[45] G. A. Alphonse and M. Toda, "Mode coupling in angled facet semiconductor optical amplifiers and superluminescent diodes," *J. Lightw. Technol.*, vol. 10, no. 2, pp. 215–219, Feb. 1992.

[46] A. Kafar *et al.*, "Design and optimization of InGaN superluminescent diodes," *Phys. Status Solidi A*, vol. 212, no. 5, pp. 997–1004, May 2015.

[47] A. Kafar *et al.*, "High optical power ultraviolet superluminescent InGaN diodes," *Proc. SPIE*, vol. 8625, 2013, Art. no. 86251S.

[48] H. Ohno *et al.*, "200mW GaN-based superluminescent diode with a novel waveguide structure," in *Proc. IEEE Photon. Conf.*, 2011, pp. 505–506.

[49] A. Kafar *et al.*, "InAlGaN superluminescent diodes fabricated on patterned substrates: an alternative semiconductor broadband emitter," *Photon. Res.*, vol. 5, no. 2, pp. A30–A34, 2017.
[50] T. Weig *et al.*, "Implementation and investigation of mode locking in GaN-based laser diodes in external cavity configuration," *Phys. Status Solidi A*, vol. 212, no. 5, pp. 986–991, May 2015.
[51] G. R. Goldberg *et al.*, "Gallium nitride light sources for optical coherence tomography," *Proc. SPIE*, vol. 10104, 2017, Art. no. 101041X.
[52] A. K. Rishinaramangalam *et al.*, "Nonpolar GaN-based superluminescent diode with 2.5 GHz modulation bandwidth," in *Proc. IEEE Int. Semicond. Laser Conf.*, 2018, pp. 133–134.
[53] A. Castiglia *et al.*, "Recent progress on GaN-based superluminescent light-emitting diodes in the visible range," *Proc. SPIE*, vol. 10532, 2018, Art. no. 105321x.
[54] C. Shen *et al.*, "Semipolar InGaN-based superluminescent diodes for solid-state lighting and visible light communications," *Proc. SPIE*, vol. 10104, 2017, Art. no. 101041u.
[55] M. Rossetti *et al.*, "3-5: RGB superluminescent diodes for AR micro-displays," *SID Symp. Dig. Techn. Papers*, vol. 49, no. 1, pp. 17–20, 2018.
[56] N. Matuschek *et al.*, "Latest improvements on RGB superluminescent LEDs," in *Proc. 18th Int. Conf. Numer. Simul. Optoelectron. Devices*, 2018, pp. 1–2.
[57] L. Wang *et al.*, "Abnormal stranski–krastanov mode growth of green InGaN quantum dots: Morphology, optical properties, and applications in light-emitting devices," *ACS Appl. Mater. Interfaces*, vol. 11, no. 1, pp. 1228–1238, 2019.
[58] S. Pimputkar *et al.*, "Prospects for LED lighting," *Nat. Photon.*, vol. 3, no. 4, pp. 180–182, Apr. 2009.
[59] J. Y. Tsao *et al.*, "Toward smart and ultra-efficient solid-state lighting," *Adv. Opt. Mater.*, vol. 2, no. 9, pp. 809–836, Sep. 2014.
[60] M. Cantore *et al.*, "High luminous flux from single crystal phosphor-converted laser-based white lighting system," *Opt. Express*, vol. 24, no. 2, pp. A215–A221, 2016.
[61] F. M. Wang, Y. H. Zhao, and N. Chi, "High speed visible light communication system using QAM-DMT modulation based on digital zero-padding and differential receiver," in *Proc. 16th Int. Conf. Opt. Commun. Netw.*, 2017.
[62] X. X. Huang *et al.*, "A Gb/s VLC transmission using hardware preequalization circuit," *IEEE Photon. Technol. Lett.*, vol. 27, no. 18, pp. 1915–1918, Sep. 15, 2015.
[63] Y. G. Wang *et al.*, "8-Gb/s RGBY LED-based WDM VLC system employing high-order CAP modulation and hybrid post equalizer," *IEEE Photon. J.*, vol. 7, no. 6, Dec. 2015, Art. no. 7904507.
[64] X. X. Huang *et al.*, "750Mbit/s visible light communications employing 64QAM-OFDM based on amplitude equalization circuit," in *Proc. Opt. Fiber Commun. Conf. Exhib.*, 2015, Art. No. 7121819.
[65] X. X. Huang *et al.*, "1.6 Gbit/s phosphorescent white LED based VLC transmission using a cascaded pre-equalization circuit and a differential outputs PIN receiver," *Opt. Express*, vol. 23, no. 17, pp. 22034–22042, 2015.
[66] J. Vucic *et al.*, "513 Mbit/s visible light communications link based on dmt-modulation of a white LED," *J. Lightw. Technol.*, vol. 28, no. 24, pp. 3512–3518, Dec. 2010.
[67] N. Chi *et al.*, "Ultra-high-speed single red-green-blue light-emitting diode-based visible light communication system utilizing advanced modulation formats," *Chin. Opt. Lett.*, vol. 12, no. 1, 2014, Art. no. 010605.
[68] Y. Q. Wang *et al.*, "Demonstration of 575-Mb/s downlink and 225-Mb/s uplink bi-directional SCM-WDM visible light communication using RGB LED and phosphor-based LED," *Opt. Express*, vol. 21, no. 1, pp. 1203–1208, 2013.
[69] F. M. Wang *et al.*, "High speed underwater visible light communication system based on LED employing maximum ratio combination with multi-PIN reception," *Opt. Commun.*, vol. 425, pp. 106–112, 2018.
[70] Z. Zhang *et al.*, "Worst-case residual clipping noise power model for bit loading in LACO-OFDM," in *Proc. Global LIFI Congr.*, 2018, pp. 1–6.
[71] C. L. Liao *et al.*, "High-speed light-emitting diodes emitting at 500 nm with 463-MHz modulation bandwidth," *IEEE Electron Device Lett.*, vol. 35, no. 5, pp. 563–565, May 2014.
[72] R. Ferreira *et al.*, "High bandwidth GaN-based micro-LEDs for multi-Gbps visible light communications," *IEEE Photon. Technol. Lett.*, vol. 28, no.19, Oct. 2016.
[73] J. W. Shi *et al.*, "III-nitride-based cyan light-emitting diodes with GHz bandwidth for high-speed visible light communication," *IEEE Electron Device Lett.*, vol. 37, no. 7, pp. 894–897, Jul. 2016.
[74] A. Rashidi *et al.*, "Nonpolar m-plane InGaN/GaN micro-scale light-emitting diode with 1.5 GHz modulation bandwidth," *IEEE Electron Device Lett.*, vol. 39, no. 4, pp. 520–523, Apr. 2018.
[75] C. Shen *et al.*, "Laser-based visible light communications and underwater wireless optical communications: a device perspective." *Proc. SPIE*, vol. 10939, 2019, Art. no. 109390E.
[76] Y. Nakatsu *et al.*, "High-efficiency blue and green laser diodes for laser displays," *Proc. SPIE*, vol. 10918, 2019, Art. no. 109181D.

Chao Shen (S'11–M'17) received the B.S. degree in materials physics from Fudan University, Shanghai, China, in 2011, and the Ph.D. degree in electrical engineering from the King Abdullah University of Science and Technology, Thuwal, Saudi Arabia, in 2017.

Since 2017, he has been a Consultant with KAUST Innovation and Economic Development, Thuwal, Saudi Arabia. He has coauthored more than 50 peer-reviewed journal and conference papers. His research interests include III-nitride laser diodes, superluminescent diodes, and micro-LEDs, as well as their applications for solid-state lighting, visible light communications, and photonic integrated circuits.

Jorge A. Holguin-Lerma (S'16) received the college degree in electromedical engineering from Universidad La Salle Chihuahua, Chihuahua, Mexico, in 2013, and the MS degree in materials science and engineering from the King Abdullah University of Science and Technology (KAUST), Thuwal, Saudi Arabia, in 2016. He is currently working toward the Ph.D. degree in photonics and optoelectronics (EE) with KAUST. He is interested in III-Nitride lasers and superluminescent diodes. He worked in the area of device characterization as a components engineer at Honeywell ACS. He is a student member of SPIE, and OSA.

Abdullah A. Alatawi (S'17) received the B.Sc. degree in aerospace engineering from the King Fahad University of Petroleum and Minerals, Dhahran, Saudi Arabia, in 2004 and the Master of Science degree in optical nanotechnology engineering from the University of Kassel, Kassel, Germany, in 2014. He is working toward the Ph.D. degree with Photonics Laboratory, King Abdullah University of Science & Technology, Thuwal, Saudi Arabia. His research interests include the study of semiconductor lasers, LEDs, and SLDs for applications in energy efficient lighting and visible light communications. The topic of his thesis covers the investigation and improvement of VCSEL devices. From 2005 to 2016, he was a Research Assistance with the Space Institute at King Abdullaziz City for Science and Technology, Riyadh, Saudi Arabia. During this time, he has the ability to manage multidisciplinary projects in the field of photonics devices.

Peng Zou received the B.S. degree in electrical engineering and automation and the M.S. degree in control engineering from Beijing University of Aeronautics and Astronautics, Beijing, China, in 2012 and 2015, respectively. He is currently working toward the Ph.D. degree in electromagnetic field and microwave technology with Fudan University, Shanghai, China. From February 2015 to December 2017, he was with the Shanghai Institute of Technical Physics, Chinese Academy of Sciences. His research interest includes visible light communication.

Nan Chi (M'03) received the B.S. and Ph.D. degrees in electrical engineering from the Beijing University of Posts and Telecommunications, Beijing, China, in 1996 and 2001, respectively. From July 2001 to December 2004, she was an Assistant Professor with the Research Center COM, Technical University of Denmark, Lyngby, Denmark. From January 2005 to April 2006, she was a Research Associate with the University of Bristol, Bristol, U.K. In June 2006, she joined Wuhan National Laboratory for Optoelectronics, Huazhong University of Science and Technology, where she was a Full Professor. In June 2008, She was with the School of Information Science and Engineering, Fudan University. She is the author or co-author of more than 200 papers. She has been the Chair of the APOC 2007 OsRT workshop and ACP 2010. She was the Technical Program Committee Member of many conferences such as APOC 08, ICAIT09, ACP 2011, WOCC 2012, ACP 2013, and IWOO 2014. Her research interests include coherent optical transmission, visible light communication, and optical packet/burst switching. She was the recipient of the New Century Excellent Talents Awards from the Education Ministry of China, Shanghai Shu Guang scholarship, Japanese OKAWA intelligence Fund Award, Pujiang talent of Shanghai City, and Ten Outstanding IT Young Persons Awards of Shanghai City.

Tien Khee Ng (SM'17) received the Ph.D. degree in 2005 and the M.Eng. degree in 2001 from Nanyang Technological University (NTU), Singapore. During 1997–1998, he was a Test Engineer at Hewlett-Packard Singapore, a Member of Technical-Staff with Tinggi Technologies (2004–2006), and a Research Fellow at NTU until 2009. He is a Senior Research Scientist with Ooi-group at King Abdullah University of Science and Technology, Thuwal, Saudi Arabia. He is also a Co-Principal Investigator responsible for innovation in MBE-grown nanostructures devices and in laser devices, at the KACST Technology-Innovation-Center at KAUST, where he realized wide-bandgap nitride quantum-confined and nanowires structures for light-emitters technology, optical wireless communications, and energy harvesting. He is a Member of SPIE, and a Senior Member of OSA.

Boon S. Ooi (M'95–SM'03) received the Ph.D. degree from the University of Glasgow, Glasgow, U.K., in 1994. He was with the King Abdullah University of Science and Technology (KAUST) from Lehigh University, Bethlehem, PA, USA, in 2009. He is currently a Professor of electrical engineering at KAUST. His recent research is concerned with the study of III-Nitride based materials and devices, and lasers for applications such as solid-state lighting, visible light and underwater wireless optical communications, and energy harvesting devices. He has served on the technical program of IEDM, ISLC, OFC, CLEO and IPC. He is currently an Associate Editor of *Optics Express* (OSA) and the IEEE PHOTONICS JOURNAL. He is a Fellow of OSA, SPIE and IoP (U.K.).